J Musculoskelet Neuronal Interact 2014; 14(4):454-463

Original Article

Hylonome

Sharpin is a key regulator of skeletal homeostasis in a TNF-dependent manner

H.W. McGowan[1], J.A. Schuijers[1], B.L. Grills[1], S.J. McDonald[1], J.A. Rickard[2], J. Silke[1,2], A.C. McDonald[1]

[1]La Trobe University, Department of Human Biosciences, La Trobe University, Bundoora, Australia;
[2]The Walter and Eliza Hall Institute, 1G Royal Parade, Parkville, Victoria 3052, Melbourne, Australia

Abstract

Objectives: SHARPIN is a subunit of LUBAC and regulates activation of NF-κB, a pivotal transcription factor in skeletal homeostasis. Mutated SHARPIN gene (*cpdm*) mice develop chronic proliferative dermatitis and systemic inflammation. *Cpdm* mice have an osteopaenic phenotype characterised by decreased cortical and trabecular bone volume, but whether this is a consequence of the hyper-inflammatory phenotype is unknown. The inflammatory phenotype of *cpdm* mice is prevented by Tnf deficiency so we examined *cpdm.Tnf* $^{-/-}$ mice to examine the role of SHARPIN in skeletal development. **Methods:** This research determined the extent to which SHARPIN and TNF interact within the skeleton through analyses of gene expression, μCT and biomechanical properties of bones of control (CTRL), *cpdm*, *Tnf* $^{-/-}$ (TNF KO) and *cpdm.Tnf* $^{-/-}$ (*cpdm*/TNF KO) mice. **Results:** Gene expression of IL-1β, TNF and caspase-3 increased in *cpdm* mice but was comparable to control values in *cpdm*/TNF KO mice. Decreased cortical and trabecular bone in *cpdm* mice translated to a loss in bone strength (ultimate stress and peak force). *Cpdm*/TNF KO mice developed bones similar to, or stronger than, control bones. **Conclusions:** Our results suggest that SHARPIN plays a significant role in skeletal homeostasis and that this role is strongly regulated through TNF pathways.

Keywords: Bone, SHARPIN, TNF, Biomechanics, Osteopaenic

Introduction

Nuclear Factor kappa-light-chain-enhancer of activated B cells (NF-κB) is a family of transcription factors essential for bone cell differentiation, function and survival[1]. These transcription factors are hetero- or homodimers constructed from 5 monomers: RelA (p65), RelB, cRel, p50 (p105) and p52 (p100)[2,3]. The two known pathways mediating the activation of NF-κB are the canonical (classical) pathway and non-canonical (alternative) pathway. Although the non-canonical pathway has been shown to be important in bone cell function (e.g osteoclastic differentiation[1]) SHARPIN, the protein of interest in this study, is involved in the canonical pathway and hence this pathway will be the focus of our discussion. SHARPIN is a component of the Linear Ubiquitin Chain Assembly Complex (LUBAC) and is essential in the regulation of normal transcription via the canonical pathway[4-7], allowing NF-κB to enter the nucleus and induce transcription of numerous inflammatory, developmental and survival genes[8]. Activation of the canonical pathway can be triggered by physical stress (e.g. ultraviolet light), the interleukin-1 (IL-1) receptor, the lipopolysaccharide receptor, T and B cell receptors and tumour necrosis factor (TNF) type 1 receptor (TNFR1)[2,5,9]. Stimulation of TNFR1 by TNF activates both pro-survival (complex I) and pro-apoptotic (complex II) signalling[10] (Figure 1A). In the absence of SHARPIN, the TNF-mediated apoptosis via complex II is upregulated[10,11] (Figure 1B). SHARPIN-deficient splenic B cells, macrophages, mouse embryonic fibroblasts and hepatocytes have all shown impaired NF-κB activation following treatment with TNF[5,12].

Mice with loss-of-function SHARPIN (*cpdm*) develop

The authors have no conflict of interest. The views expressed in this manuscript are those of the authors and not an official position of La Trobe University.

Corresponding author: Aaron McDonald, PhD. La Trobe University | Department of Human Biosciences | Faculty of Health Sciences | Health Sciences Building 2 | Room 437 | La Trobe University | Bundoora 3086 | VIC | Australia

E-mail: A.McDonald@latrobe.edu.au

Edited by: M. Hamrick
Accepted 22 October 2014

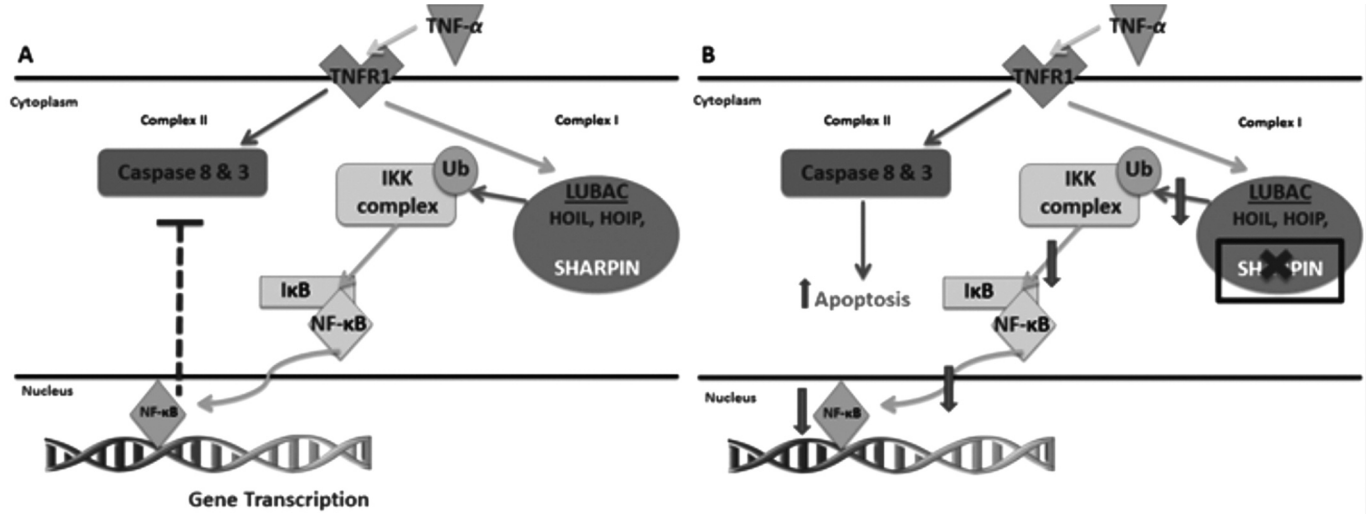

Figure 1. TNFR1 canonical pathway. (A) Upon TNFR1 activation linear ubiquitin chain assembly complex (LUBAC) linearly ubiquitylates (Ub) RIPK1 and NEMO/IKKγ leading to activation of the, NEMO containing, inhibitor of kappaB-kinase (IKK) complex. The IKK complex phosphorylates inhibitor of kappaB (IκB) to release NF-κB for translocation into the nucleus (Complex I). This results in both gene transcription and inhibition of apoptosis (Complex II). (B) Loss-of-function sharpin (X) in LUBAC decreases the sequence of events outlined in (A) leading to impaired translocation (↓) of NF-κB via Complex I and increased TNF-induced apoptosis (↑) via Complex II.

chronic proliferative dermatitis, multiple organ inflammation (including oesophagus, lung and liver), absence of Peyer's patches, splenomegaly and abnormal lymphoid architecture[5,13]. The *cpdm* phenotype is initially recognized as erythematous, scaly areas of alopecia at 3-4 weeks of age. Recently *cpdm* mice have also been identified as having skeletal abnormalities[14]. Specifically, Xia and associates found that the metaphysis of *cpdm* mice femora showed a decrease in gene expression for the osteoblastic markers Runt-related transcription factor 2 (Runx2), osteocalcin, osterix and collagen type I[14]. When bone marrow stromal cells of *cpdm* mice were cultured *ex vivo*, there was no difference in osteoblastic proliferation however bone mineral formation and osteoclastic formation and function decreased compared with wild-type[14].

TNF is a known regulator of both osteoclasts and osteoblasts, and TNFR1 is the functional form of the receptor for both these cells types[15]. TNF, acting via TNFR1, promotes osteoclastogenesis[16] and several studies identify the capacity of TNF to directly stimulate osteoclastogenesis, even in the absence of receptor activator of nuclear factor-kappa B ligand (RANKL)[17-19]. Osteoblastogenesis, on the other hand, is inhibited by TNF[20-22]. It may therefore be predicted that SHARPIN might play a downstream role in TNFR1 activation to stimulate osteoclastogenesis, inhibit osteoblastogenesis or both. While TNF alters the activity and differentiation of osseous cells, the skeletal phenotypes of *Tnfr1*$^{-/-}$ and *Tnfr2*$^{-/-}$ mice are grossly normal[15,23].

Although SHARPIN mRNA is present in mouse osteoblasts and osteoclasts (http://biogps.org) the pathway(s) in which SHARPIN is involved in regulation of osseous cells has yet to be determined. The hyper-inflammatory phenotype of *cpdm* mice is corrected by crossing with *Tnf*$^{-/-}$ mice[10,24]. It was therefore of interest to determine if the TNF – LUBAC – NF-κB pathway plays a role in osseous cell formation and function or if the skeletal abnormalities seen in *cpdm* mice were due to an alternative pathway.

Materials and methods

Genetically modified mice and tissue processing

Tnf$^{-/-}$ mice were a gift from H. Körner[25], while *cpdm* mice were obtained from The Jackson Laboratory (CA, USA). Colonies were kept under conventional conditions. *Cpdm* mice were crossed with *Tnf*$^{-/-}$ mice and typed by PCR and sequencing[7]. All mice were male between the ages of 12-16 weeks.

All bones were collected following cervical dislocation. The right femur was stored in RNAlater (Sigma-Aldrich) at -80°C prior to RT-qPCR analysis. The left femur was fixed 4% paraformaldehyde and stored in ethanol at 4°C prior to micro-computed tomography analysis. The right humerus was stored in silicone oil, at -20°C prior to biomechanical analysis.

RT-qPCR

Approximately 200 μg of proximal whole femur was snap-frozen in liquid nitrogen, homogenised with PureZOL and RNA extracted using the Bio-Rad Aurum™ Total RNA Fatty and Fibrous Tissue Kit using the supplied protocol (Bio-Rad Laboratories), with purity of RNA validated with $A_{260/280}$ ratios using a NanoDrop 2000 (Thermo Scientific). Resulting samples were reverse transcribed to cDNA using the iScript Select cDNA Synthesis Kit (Bio-Rad Laboratories). qPCR was run over 55 cycles using the iCycler iQ Multi-Colour Real Time PCR detection sys-

Gene	Forward Sequence	Reverse Sequence
TNF-α[27]	5'TTGCTTCTTCCCTGTTCC 3'	5'CTGGGCAGCGTTTATTCT3'
IL-1β[28]	5'CATTGTGGCTGTGGAGAAG3'	5'ATCATCCCACGAGTCACAGA3'
OPG[29]	5'GCCAACACTGATGGAGCAGAT3'	5'TCTTCATTCCCACCAACTGATG3
RANKL[29]	5'GCTCACCTCACCATCAATGCT3'	5'GGTACCAAGAGGACAGACTGACTTTA3'
Cathepsin K	5'CCATATGTGGGCCAGGATG3'	5'AGGAATCTCTCTGTACCCTCTGCA3'
Collagen I (COLIα1)	5'CCTGGTCCTCACGGTTCTG3'	5'TGTCACCTCGGATGCCTTG3'
Caspase-3	5'TCTGACTGGAAAGCCGAAACTC3'	5'TCCCACTGTCTGTCTCAATGCCAC3'
Reference Gene		
β-actin[27]	5'ATTGTAACCAACTGGGACG3'	5'TCTCCAGGGAGGAAGAGG3'

Table 1. Primer sequences.

tem (using SsoFast EvaGreen) with melt-curve analysis performed post-cycling to establish specificity of DNA products. The primer sequences for genes of interest are shown in Table 1. Primer sequences were prepared commercially by GeneWorks Pty Ltd (Adelaide, Australia) from previous publications or determined using the PubMed genome sequence search (GenBank) and primers designed using the Beacon Designer 2.0 software (Biosoft International, PaloAlto, CA, USA). β-actin was used as an internal reference for each sample. Using the Pfaffl method[26], gene expression was normalised to the β-actin mRNA level and presented as relative expression.

The volume of reagents in each well-plate consisted of: SsoFast Eva Green Supermix (10 μL), forward primer (1.5 μL), reverse primer (1.5 μL), RNase-free H2O (5 μL), cDNA (5 μL) (total 23.0 μL). PCR was run over 55 cycles using the CFX-96 Multi-Colour Real Time PCR detection system with melt-curve analysis performed post-cycling to confirm specificity of DNA products.

Microcomputed tomography analysis (μCT)

Three-dimensional (3D) bone images of femora from all groups were generated. This was performed using the microcomputed tomography (micro-CT) scanner SkyScan 1076 (Kontich, Belgium). Both trabecular and cortical bone were investigated with 1373 slices (9.06 μm thick). Scanning was conducted at 50kV and 100 μA (using a 0.5 mm aluminium filter and rotation step of 0.5 degrees) with a spatial resolution of approximately 9 μm/pixel. Images were reconstructed using NRecon, aligned with DataViewer software and calculation of structural indices performed using a 3D image analysis system, CTAn software. Analysis included trabecular bone volume fraction (BV/TV %), trabecular thickness (Tb.Th, mm), trabecular separation (Tb.Sp, mm), trabecular number (Tb,N. 1/mm), cortical thickness (mm), cortical volume (mm3) and mean polar moment of inertia (mm^4).

Bone biomechanics

Bone samples, stored in silicone oil, at -20°C were thawed 1 h prior to experimentation. The cortical bone strength of the mid-shaft mouse humerus was tested using a three-point bending apparatus attached to a PC with the Crusher 3-point bending software installed (La Trobe University Technical Support, Australia). The apparatus consisted of a transducer set at 50 lb sampling at a rate of 100 samples/sec, with calibration performed using a series of masses up to 600 g. Bones were individually removed from silicon oil and cleaned with paper towel. Humeri were centrally placed over the testing platform consisting of two posts separated by 5.6 mm, with the deltoid tuberosity placed between the platforms and facing inferiorly. Bones were loaded at a rate of 1 mm/sec until fracture occurred or the force lever reached its maximum displacement. Displacement (mm) and force (N) data were recorded continuously. Fractured surfaces of both ends of biomechanically tested bones were imprinted into dental wax. Wax sections were viewed under a Leica Microsystems DM-RBE microscope at 25x magnification attached to a Leica DFC490 camera, with cortical bone measured by analysis of outer (A_o), inner (A_i), and total (A_t) bone areas under Leica Image Manager software. These values were then used to determine Young's Modulus (the intrinsic stiffness), determined by $E=(F/Y) \times (\pi L^3/12(A_o^2-A_i^2)$; and ultimate tensile stress (the maximum stress which can be applied to the bone prior to fracture), determined by $\sigma=(F.L.A_t^{1/2})/(\pi^{1/2}(A_o^2-A_i^2))$, where F is the peak force applied to the bone, F/Y is the slope of the force/displacement curve, L is the distance between the testing platforms (.0056 m), A_o is the outside cross-sectional area (m^2), A_t is the total cortical bone volume (m^2), A_i is the internal cross-sectional area of the bone (m^2) and σ is the ultimate tensile stress (N/m^2)[30].

Statistical analysis

All values have been expressed as mean ± standard error of the mean (S.E.). Statistical analyses were undertaken using GraphPad Prism 5 software. A one-way ANOVA was performed with post-hoc Neuman-Keuls analysis to determine statistical significance between all 4 groups. A Students' t-test was performed between CTRL and *cpdm* groups for TNF gene expression. Values of $p<0.05$ were considered statistically significant.

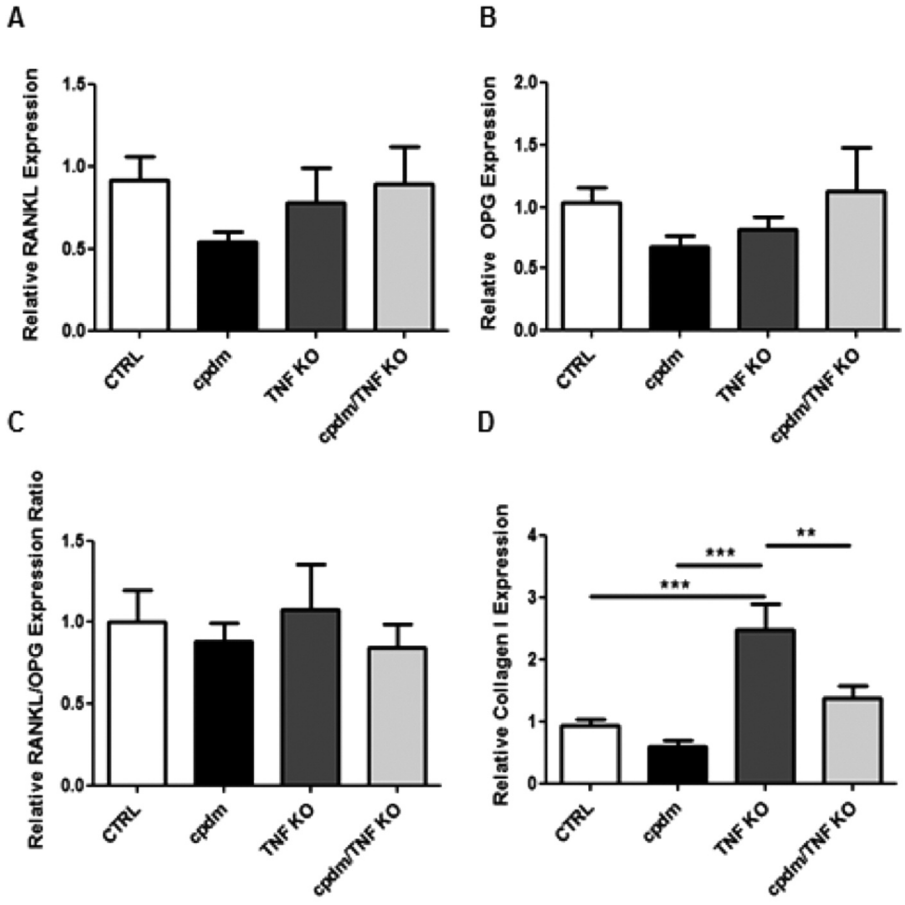

Figure 2. RT-qPCR analysis of proximal femur of control (CTRL), loss-of-function SHARPIN (*cpdm*), *Tnf* $^{-/-}$ (TNF KO) and *cpdm*/TNF KO mice. There was no significant change in RANKL expression (A) OPG expression (B) or the OPG/RANKL expression ratio (C). Collagen I expression (D) increased significantly in TNF KO mice compared with CTRL (***p<0.005), *cpdm* (***p<0.005) and *cpdm*/TNF KO (**p<0.01) groups. (means±S.E.) (n=6).

Results

RT-qPCR

Figure 2 shows the results of the qPCR analysis of CTRL, *cpdm*, TNF KO and *cpdm*/TNF KO mice for RANKL, osteoprotegerin (OPG), RANKL/OPG RNA expression ratio and collagen type I expression. Although there was no significant change in either RANKL expression (Figure 2A) or OPG expression (Figure 2B) our results indicated a trend toward a decrease in both genes in *cpdm* versus CTRL mice. Expression of both of these genes also indicated a trend toward normal CTRL values in both the TNF KO and *cpdm*/TNF KO groups. As indicated, there was no significant difference in the RANKL/OPG RNA expression ratio between groups (Figure 2C). There was again a trend toward a decrease in collagen I expression in *cpdm* versus CTRL mice (Figure 2D). Collagen I expression was significantly higher in TNF KO mice compared with *cpdm* (p<0.005), *cpdm*/TNF KO (p<0.01) and the CTRL group (p<0.005).

Figure 3 shows the results of the qPCR analysis of CTRL, *cpdm*, TNF KO and *cpdm*/TNF KO mice for IL-1β, cathepsin K, caspase-3 expression and results of the qPCR analysis of CTRL compared with *cpdm* mice for TNF expression (no TNF PCR products were detected in both the TNF KO and the *cpdm*/TNF KO groups). *Cpdm* and TNF KO mice showed an almost two-fold increase in IL-1β expression compared with CTRL mice (p<0.05 for both) and *cpdm*/TNF mice (p<0.01 for both) (Figure 3A). Figure 3B shows a significant increase in TNF expression in the *cpdm* group compared with CRTL (p<0.05). Figure 3C shows a trend toward a decrease in cathepsin K expression in *cpdm* mice compared with CTRL mice. Cathepsin K expression increased in both TNF KO and *cpdm*/TNF mice versus *cpdm* mice (p<0.05 for both). These results indicated a return to normal cathepsin K expression values in both the TNF KO and *cpdm*/TNF KO groups. There was a significant (p<0.01) increase in caspase-3 expression in *cpdm* mice compared with CTRL mice (p<0.01; Figure 3D). Caspase-3 expression also showed a return to normal values as expression had decreased significantly in both TNF KO and *cpdm*/TNF KO mice compared with *cpdm* mice (p<0.05 and p<0.01 respectively; Figure 3D).

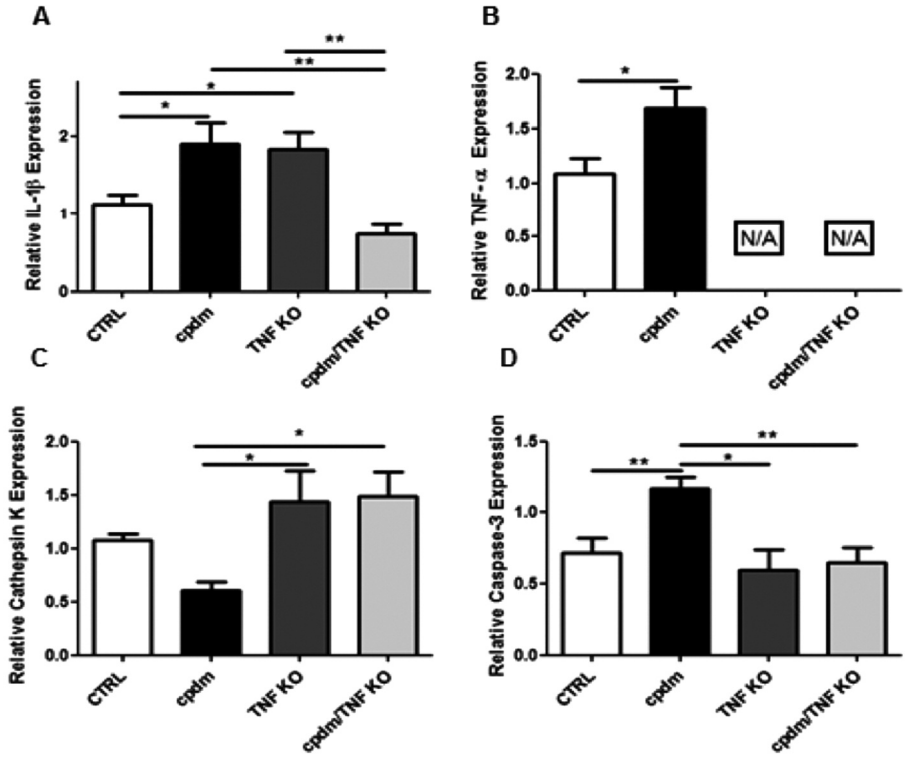

Figure 3. RT-qPCR analysis of proximal femur of control (CTRL), loss-of-function sharpin (*cpdm*), TNF knockout (TNF KO) and *cpdm*/TNF KO mice. (A) Increased IL-1β expression in *cpdm* and TNF KO mice compared with CTRL (*p<0.05) and *cpdm*/TNF KO mice (**p<0.01). (B) TNF expression in *cpdm* mice increased relative to the CTRL group (*p<0.05). N/A indicating no TNF products detected in either TNF KO or *cpdm*/TNF KO mice. (C) Increased cathepsin K expression in TNF KO and *cpdm*/TNF KO compared with *cpdm* mice (*p<0.05). (D) A significant increase in caspase-3 expression in *cpdm* mice compared with the CTRL (**p<0.01), TNF KO (*p<0.05) and *cpdm*/TNF KO (**p<0.01) groups (**p<0.01). (means±S.E.) (n=5).

μCT

Figure 4 shows the results of the μCT trabecular analysis of the distal femur of CTRL, *cpdm*, TNF KO and *cpdm*/TNF KO mice. There was a significant (p<0.01) decrease in trabecular bone volume in *cpdm* mice (10.97±0.56 %BV/TV) compared with CTRL mice (23.87±3.66% BV/TV). TNF KO (25.33±3.07% BV/TV) and *cpdm*/TNF KO (23.88±1.5% BV/TV) mice showed a significantly increased BV/TV (p<0.01 for both) compared with *cpdm* mice, showing a bone volume comparable to control bones. Trabecular thickness (Tb.Th) was decreased in *cpdm* mice (0.06±0.001 mm) compared with CTRL animals (0.07±0.002 mm) (p<0.05) while TNF KO (0.07±0.003 mm) and *cpdm*/TNF KO mice (0.07±0.001 mm) showed a significantly increased Tb.Th compared with *cpdm* mice (p<0.01 for both). There was a significant (p<0.05) decrease in trabecular number in *cpdm* mice (1.89±0.08 1/mm) compared with CTRL mice (3.52±0.52 1/mm) while TNF KO (3.58±0.35 1/mm) and *cpdm*/TNF KO mice (3.43±0.22 1/mm) showed a significantly increased Tb.N compared with *cpdm* mice (p<0.01 for both). Furthermore, trabecular separation (Tb.Sp) was also increased (p<0.01) in *cpdm* animals (0.24±0.01 mm) compared with CTRL animals (0.16±0.02 mm) while TNF KO (0.17±0.02 mm) and *cpdm*/TNF KO mice (0.16±0.01 mm) showed a significantly decreased Tb.Sp compared with *cpdm* mice (p<0.01 for both). All of these results indicated that trabecular bone was affected in mice with a loss-of-function sharpin gene but not in mice lacking TNF or both SHARPIN and TNF.

Figure 5 shows the cortical results of the μCT analysis of the mid-femur of CTRL, *cpdm*, TNF KO and *cpdm*/TNF KO mice. There was a significant (p<0.01) decrease in cortical bone volume in *cpdm* mice (0.12±0.02 mm^3) compared with CTRL (0.37±0.08 mm^3) while TNF KO (0.30±0.05 mm^3) and *cpdm*/TNF KO animals (0.28±0.02 mm^3) showed increased cortical volume compared with *cpdm* mice (p<0.05 for both) (Figure 5A). No significant difference in periosteal circumference was recorded between the groups (Figure 5B). Mean polar moment of inertia, which relates to the distribution of material around the centre of a specimen, and detects the resistance of long bones to torque[31] (Figure 5C) decreased (p<0.005) in *cpdm* mice (0.29±0.02 mm^4) compared with CTRL (0.53±0.06 mm^4), while increases in mean polar moment of inertia were seen in TNF KO (0.42±0.04 mm^4) (p<0.05) and *cpdm*/TNF KO (0.44±0.03 mm^4) (p<0.01 and p<0.005 respectively) compared

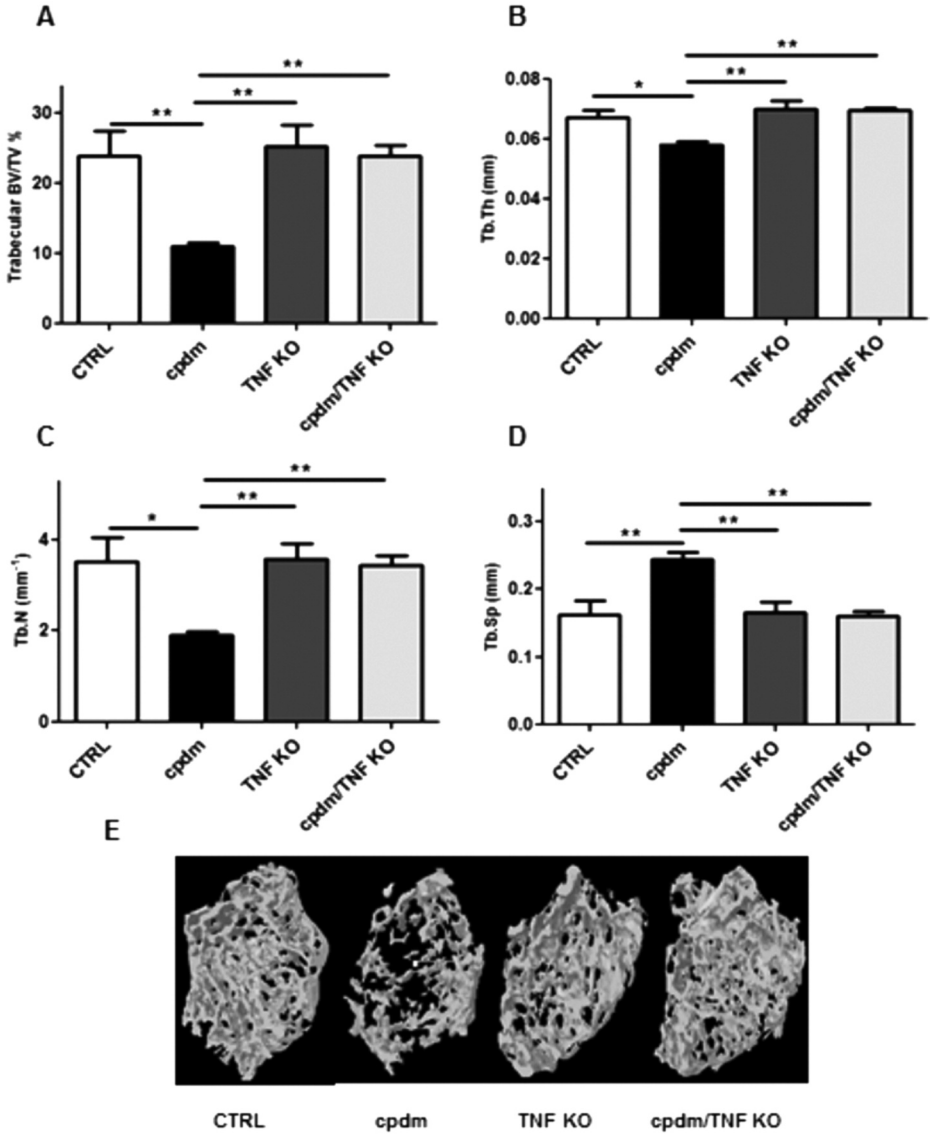

Figure 4. μCT analysis of distal femur of control (CTRL), loss-of-function sharpin (*cpdm*), TNF knockout (TNF KO) and *cpdm*/TNF KO mice. Results indicate a decrease in (A) trabecular bone volume/total volume (trabecular BV/TV %), (B) trabecular thickness (Tb.Th) and (C) trabecular number (Tb.N) for *cpdm* mice compared with CTRL mice. Trabecular BV/TV %, Tb.Th. and TB.N significantly increased in TNF KO and *cpdm*/TNF KO groups compared with *cpdm* mice (*p<0.05; **p<0.01) (n=4). There was a significant increase in (D) trabecular separation (Tb.Sp) in *cpdm* mice compared with CTRL, TNF and *cpdm*/TNF KO groups (**p<0.01). (means±S.E.) (n=4). (E) representative photos of trabecular bone of all 4 groups.

with *cpdm* mice. These results again indicated that mice with a loss-of-function SHARPIN gene had inferior structural and mechanical integrity compared with CTRL mice and mice lacking TNF or both SHARPIN and TNF.

Biomechanics

Figure 6 shows the results of biomechanical testing of the humerus of CTRL, *cpdm*, TNF KO and *cpdm*/TNF KO mice. As indicated in Figure 6A, there was a significant (p<0.05) decrease in ultimate stress in *cpdm* mice (112.9±13.0 MPa) compared with CTRL (235.2±16.3 MPa). The ultimate stress of the TNF KO group (332.3±29.7 MPa) and *cpdm*/TNF KO group (239.3±51.1 MPa) was significantly higher than the *cpdm* group (p<0.01 and p<0.05 respectively).

The *cpdm* group had a lower peak force to failure (9.6±1.6 N) than all other groups: CTRL (21.4±1.0 N; p<0.005); TNF KO (29.1±1.9 N; p<0.005); *cpdm*/TNF KO (31.5±1.5 N; p<0.005) (Figure 6B). Both the TNF KO and *cpdm*/TNF KO groups were also significantly higher than the CTRL group (p<0.01 & p<0.005 respectively).

Young's modulus results (Figure 6C) showed TNF KO

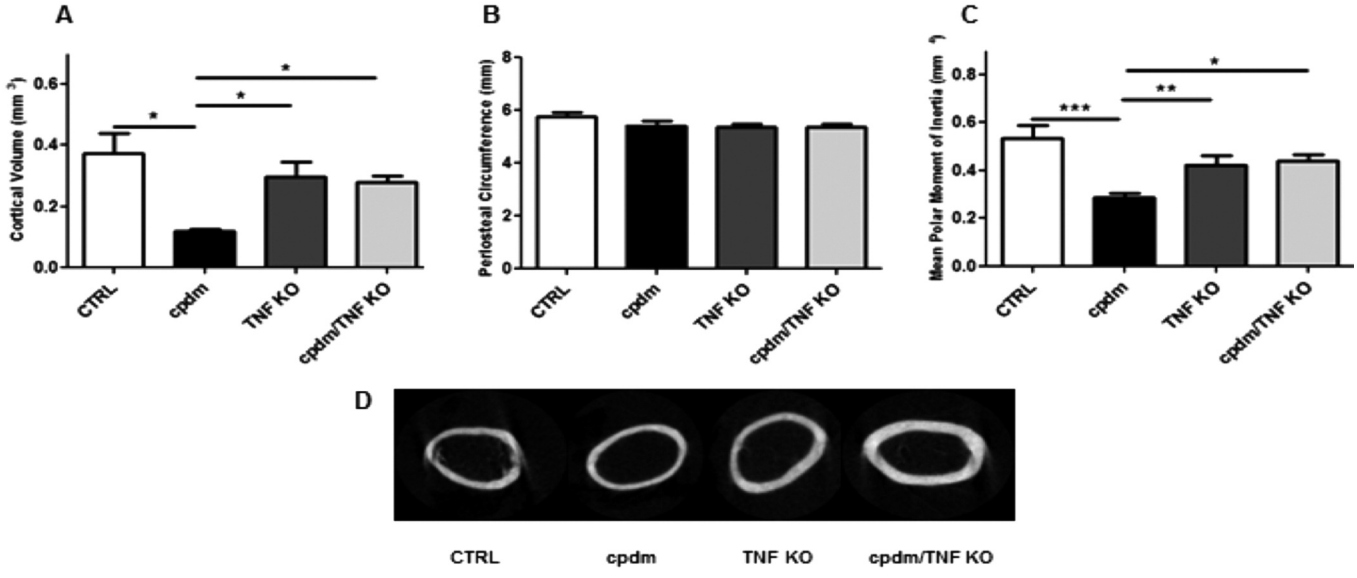

Figure 5. μCT analysis of mid-femur of control (CTRL), loss-of-function sharpin (*cpdm*), TNF knockout (TNF KO) and *cpdm*/TNF KO mice. Results indicated a decrease in (A) cortical volume and (C) mean polar moment of inertia for *cpdm* mice compared with CTRL, TNF KO and *cpdm*/TNF KO mice (*p<0.05, **p<0.01, ***p<0.005). (B) indicated no significant difference in periosteal circumference between the groups. (means±S.E.) (n=4). (D) Representative μCT photos of cortical bone of all groups.

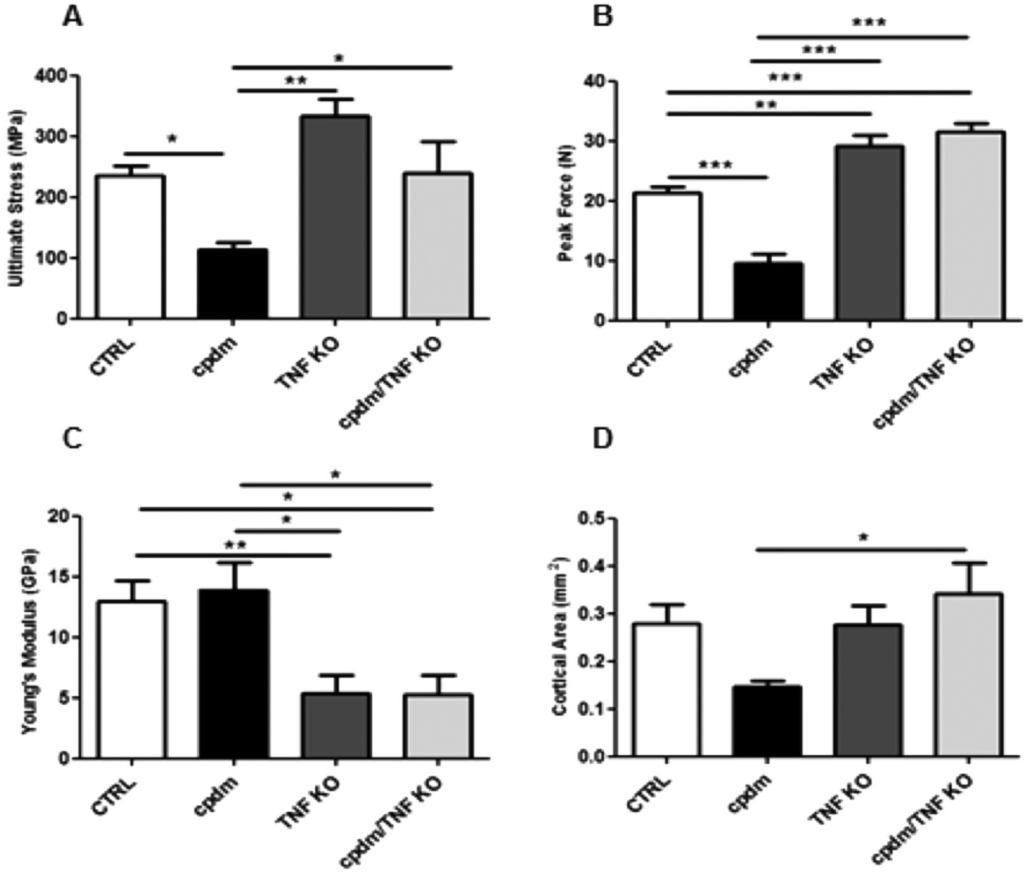

Figure 6. Biomechanical analysis of humerus of control (CTRL), loss-of-function SHARPIN (*cpdm*), TNF knockout (TNF KO) and *cpdm*/TNF KO mice. Results indicate a decrease in (A) ultimate stress, (B) peak force and (D) cortical area for *cpdm* mice compared with CTRL. These values returned to CTRL values (or higher) in the TNF KO and *cpdm*/TNF KO groups (*p<0.05, **p<0.01, ***p<0.005). Young's modulus (C) was significantly lower in TNF and *cpdm*/TNF groups compared with both CTRL and *cpdm* groups (*p<0.05, **p<0.01). (means±S.E.) (n=5).

(5.4±1.4 GPa) and *cpdm*/TNF KO (5.3±1.6 GPa) had decreased intrinsic stiffness compared with the CTRL group (13.0±1.7 GPa; $p<0.01$ and $p<0.05$ respectively) and the *cpdm* group (13.9±2.2 GPa; $p<0.05$ for both).

Results for measurements of the cortical area (Figure 6D) of the humerus showed a similar distribution to the μCT analysis of the mid-femur (Figure 5A), however there was only a significant difference recorded between the *cpdm* (0.15 mm^2 ± 0.01 mm^2) and *cpdm*/TNF KO (0.34 mm^2 ± 0.07 mm^2) groups ($p<0.05$). CTRL (0.28 mm^2 ± 0.04 mm^2) and TNF KO (0.28 mm^2 ± 0.04 mm^2) did not significantly differ.

Discussion

Cpdm mice homozygous for the *cpdm* spontaneous mutation (loss-of-function SHARPIN) develop a severe, chronic, inflammatory skin disease beginning at 3-5 weeks of age. Mice have a runted appearance and life span is shortened. In addition to dermatitis, homozygote mutants exhibit multi-organ inflammation with eosinophilia, splenomegaly, diminished serum immunoglobulins, and an absence of B cell follicles, follicular dendritic cells, and germinal centres in secondary lymph organs[32,33]. A comparative study by Xia and colleagues in 2011[14] found that *cpdm* animals exhibited osteopaenia including reduced cortical and trabecular bone volume and density compared with wild-type littermates. PCR and histochemical analyses also indicated functionally defective osteoblasts and osteoclasts. Our results support the work of Xia and colleagues, with both trabecular bone measurements and cortical bone volume decreasing in *cpdm* mice compared with controls. Our additional research of TNF KO and *cpdm*/TNF KO mice suggests that this decrease in bone may be due to the presence of TNF, as both groups lacking the TNF gene had a skeletal morphology similar to that of control mice.

Bone remodelling is tightly controlled by inflammatory and anti-inflammatory cytokines, which influence the differentiation of mononuclear cells into bone-resorbing osteoclasts[34]. The *cpdm* mutation is associated with increased inflammation and this is reflected in our study by the heightened gene expression levels of inflammatory cytokines IL-1β and TNF. Osteoclastogenesis is predominantly regulated via receptor activator of NF-κB ligand (RANKL). TNF closely regulates RANK/RANKL-induced osteoclastogenesis via TNFR1[35]. Essential for the survival and differentiation of the osteoclast, NF-κB activity is one of the first signs of osteoclastic differentiation following RANKL binding[36]. As SHARPIN is a known downstream regulator of TNFR1 activation, and our results indicate a trend toward a decrease in RANKL expression in *cpdm* mice, we postulate that SHARPIN is involved in the TNF-induced expression of RANKL and thus osteoclastogenesis. There was also a trend indicating a decrease in expression of cathepsin K, a marker for osteoclastic maturation, in *cpdm* mice compared with CTRL mice, and also a significant decrease compared with TNF and *cpdm*/TNF KO mouse groups. This suggests a role of SHARPIN in TNF-regulated, RANKL-induced osteoclastogenesis. Although osteoclastic gene expression in *cpdm* mice was not investigated by Xia and colleagues[14], our results support their previous findings proposing a decrease in osteoclastic formation and function in *cpdm* mice. The loss of TNF in our knockout animals displayed a normal bone phenotype as seen in both μCT and biomechanical analyses. This correlates to previous findings, which showed that the skeletal phenotypes of *Tnfr1*$^{-/-}$ and *Tnfr2*$^{-/-}$ mice are normal[15,23]. This indicates that SHARPIN seems to have a role in regulating the effects of TNF on osteoclastic activity, most likely via the transcription factor NF-κB.

Recent research has brought to light the complex nature of NF-κB's relationship with bone cells. NF-κB has been shown to stimulate osteoclastic activity[37] and inhibit osteoblasts[38]. In contrast, NF-κB has also been reported to have a pro-survival role in osteoblasts and its inhibition induced apoptosis in these cells[39]. As analysis of this data was performed between all four groups there was no statistically significant decrease in RANKL, OPG and collagen I expression between CTRL and *cpdm* groups. The results do, however, indicate a trend which should not be disregarded. The above three genes are all expressed by osteoblasts, which indicates that osteoblastic activity has possibly decreased (which is supported by decreased trabecular and cortical bone volume data) in *cpdm* mice. This may be due to possible increases in TNF levels in *cpdm* mice, as indicated through TNF gene expression levels. TNF is a known inhibitor of osteoblastic differentiation[40] and it may be postulated that in the absence of SHARPIN, the inhibitory effects on osteoblasts increases. Collagen I expression levels also increased significantly in TNF KO mice, but not *cpdm*/TNF KO mice, which further suggests that TNF plays an important part in negative regulation of osteoblasts, most likely controlled along the SHARPIN pathway. An alternate or additional consideration for the decrease in bone formation in *cpdm* mice is that these effects may be due to apoptosis of osteoblasts. Caspase-3 expression levels were significantly higher in *cpdm* mice compared with all other groups. As proposed in Figure 1, TNF may have stimulated the apoptotic pathway in *cpdm* osteoblasts. Our findings, in addition to those of Xia and colleagues[14], support the role of SHARPIN in osteoblastic survival and suggest further research must be performed to determine the role of the TNF-LUBAC-NF-κB pathway in both osteoblastic and osteoclastic function and survival.

Osteopetrosis occurs when osteoblastic activity exceeds osteoclastic activity[41], while osteopaenia and osteoporosis result when osteoclastic activity outweighs osteoblastic activity[42]. The loss of both cortical and trabecular bone show that *cpdm* animals display an osteopaenic phenotype. Besides bone size, bone strength depends upon bone mineral density (BMD), cortical porosity and accumulated microcracks, although geometrical measures such as bone size, cross-sectional area or area moment of inertia have frequently shown to predict up to 70–80% of whole bone strength[43]. This is reflected in the decreased peak force that *cpdm* humeri were able to withstand. Peak force is an extrinsic property of bone, and is reliant on the trabecular and cortical bone volume[44]. As such, peak force can be used to determine the overall effect of a treatment regimen or pheno-

type, but is unable to predict the overall quality of the bone microarchitecture. To determine bone quality, it is necessary to look at the intrinsic qualities of bone, such as ultimate stress. Ultimate stress is decreased in *cpdm* mice, which indicates that not only is SHARPIN responsible for causing a normal bone volume, but that SHARPIN-deficient mice have poor bone tissue quality and microarchitecture. Both TNF KO and *cpdm*/TNF KO groups had ultimate stress levels similar to controls and peak force values significantly higher. This indicates that the decrease in biomechanical properties of *cpdm* bones is due to TNF. Young's Modulus is an intrinsic measure of a bone's stiffness. Control and *cpdm* mice showed the same stiffness, while both TNF KO and *cpdm*/TNF KO groups showed a decreased stiffness. This is inconsistent with other findings in our study, which demonstrated that *cpdm* bones were greatly inferior to control bones, although it is important to distinguish stiffness, the load needed to cause minor deformation, from strength, the ability to resist fracture[45]. We hypothesised that the loss of bone in *cpdm* mice was TNF-dependent. This was supported as mice lacking the TNF gene had biomechanical properties similar to those of control mice.

Conclusion

These experiments indicated that the osteopaenia displayed in SHARPIN-deficient *cpdm* mice was alleviated by the loss of functional TNF. Removal of the TNF gene restored osteoblastic and osteoclastic gene expression to control levels, and also prevented cortical and trabecular bone loss. Despite data suggesting a potential role for TNF in skeletal development, *Tnf* $^{-/-}$ mice had bones with normal physical properties. Because systemic inflammation was prevented in *cpdm.Tnf* $^{-/-}$ mice, this strongly suggested that defects in skeletal development observed in *cpdm* mice were driven by the inflammatory cytokine milieu rather than due to a direct disruption of bone development in *cpdm* mice.

Acknowledgements

The authors would like to acknowledge the support from the Department of Human Biosciences, La Trobe University, in the award of a departmental grant. We thank Heinrich Körner for Tnf $^{-/-}$ *mice. This work was supported by NHMRC grants (1025594, 1046984) and an NHMRC fellowship to JSilke (541901).*

References

1. Novack DV. Role of NF-kappaB in the skeleton. Cell Res 2011;21(1):169-82.
2. Wajant H, Scheurich P. TNFR1-induced activation of the classical NF-kappaB pathway. Febs J 2011;278(6):862-76.
3. Xiao M, Inal CE, Parekh VI, Li XH, Whitnall MH. Role of NF-kappaB in hematopoietic niche function of osteoblasts after radiation injury. Exp Hematol 2009;37(1):52-64.
4. Tokunaga F. Linear ubiquitination-mediated NF-kappaB regulation and its related disorders. J Biochem 2013;154(4):313-23.
5. Wang Z, Potter CS, Sundberg JP, Hogenesch H. SHARPIN is a key regulator of immune and inflammatory responses. J Cell Mol Med 2012;16(10):2271-9.
6. Tokunaga F, Iwai K. LUBAC, a novel ubiquitin ligase for linear ubiquitination, is crucial for inflammation and immune responses. Microbes Infect 2012;14(7-8):563-72.
7. Gerlach B, Cordier SM, Schmukle AC, Emmerich CH, Rieser E, Haas TL, et al. Linear ubiquitination prevents inflammation and regulates immune signalling. Nature 2011;471(7340):591-6.
8. Vincent Feng-Sheng S, Rachel T, Andrew C, Alexander H. A single NFκB system for both canonical and non-canonical signaling. Cell Res 2010;21(1):86-102.
9. Tokunaga F, Iwai K. Linear ubiquitination: A novel NF-kappaB regulatory mechanism for inflammatory and immune responses by the LUBAC ubiquitin ligase complex [Review]. Endocr J 2012;59(8):641-52.
10. Silke J. The regulation of TNF signalling: what a tangled web we weave. Curr Opin Immunol 2011;23(5):620-6.
11. Ikeda F, Deribe YL, Skanland SS, Stieglitz B, Grabbe C, Franz-Wachtel M, et al. SHARPIN forms a linear ubiquitin ligase complex regulating NF-kappaB activity and apoptosis. Nature 2011;471(7340):637-41.
12. Sieber S, Lange N, Kollmorgen G, Erhardt A, Quaas A, Gontarewicz A, et al. Sharpin contributes to TNFalpha dependent NFkappaB activation and anti-apoptotic signalling in hepatocytes. PLoS ONE 2012;7(1):e29993.
13. Liang Y, Sundberg JP. SHARPIN regulates mitochondria-dependent apoptosis in keratinocytes. J Dermatol Sci 2011;63(3):148-53.
14. Xia T, Liang Y, Ma J, Li M, Gong M, Yu X. Loss-of-function of SHARPIN causes an osteopenic phenotype in mice. Endocrine 2011;39(2):104-12.
15. Nanes MS. Tumor necrosis factor-alpha: molecular and cellular mechanisms in skeletal pathology. Gene 2003;321:1-15.
16. Zhang YH, Heulsmann A, Tondravi MM, Mukherjee A, Abu-Amer Y. Tumor necrosis factor-alpha (TNF) stimulates RANKL-induced osteoclastogenesis via coupling of TNF type 1 receptor and RANK signaling pathways. J Biol Chem 2001;276(1):563-8.
17. Azuma Y, Kaji K, Katogi R, Takeshita S, Kudo A. Tumor necrosis factor-alpha induces differentiation of and bone resorption by osteoclasts. J Biol Chem 2000;275(7):4858-64.
18. Kim N, Kadono Y, Takami M, Lee J, Lee S-H, Okada F, et al. Osteoclast differentiation independent of the TRANCE-RANK-TRAF6 axis. J Exp Med 2005; 202(5):589-95.
19. Kobayashi K, Takahashi N, Jimi E, Udagawa N, Takami M, Kotake S, et al. Tumor necrosis factor alpha stimulates osteoclast differentiation by a mechanism independent of the ODF/RANKL-RANK interaction. J Exp Med 2000; 191(2):275-86.
20. Tsukasaki M, Yamada A, Suzuki D, Aizawa R, Miyazono

A, Miyamoto Y, et al. Expression of POEM, a positive regulator of osteoblast differentiation, is suppressed by TNF-alpha. Biochem Biophys Res Commun 2011; 410(4):766-70.
21. Gilbert LC, Chen H, Lu X, Nanes MS. Chronic low dose tumor necrosis factor-alpha (TNF) suppresses early bone accrual in young mice by inhibiting osteoblasts without affecting osteoclasts. Bone 2013;56(1):174-83.
22. Li Y, Li A, Strait K, Zhang H, Nanes MS, Weitzmann MN. Endogenous TNFalpha lowers maximum peak bone mass and inhibits osteoblastic Smad activation through NF-kappaB.[Erratum appears in J Bone Miner Res 2007 Jun;22(6):949]. J Bone Miner Res 2007;22(5):646-55.
23. Vargas SJ, Naprta A, Lee SK, Kalinowski J, Kawaguchi H, Pilbeam CC, et al. Lack of evidence for an increase in interleukin-6 expression in adult murine bone, bone marrow, and marrow stromal cell cultures after ovariectomy. J Bone Miner Res 1996;11(12):1926-34.
24. Iwai K. Linear polyubiquitin chains: a new modifier involved in NFkappaB activation and chronic inflammation, including dermatitis. Cell Cycle 2011;10(18):3095-104.
25. Korner H, Cook M, Riminton DS, Lemckert FA, Hoek RM, Ledermann B, et al. Distinct roles for lymphotoxin-alpha and tumor necrosis factor in organogenesis and spatial organization of lymphoid tissue. European journal of immunology 1997;27(10):2600-9.
26. Pfaffl MW. A new mathematical model for relative quantification in real-time RT-PCR. Nucleic Acids Res 2001; 29(9):e45.
27. Liu N, Chen R, Du H, Wang J, Zhang Y, Wen J. Expression of IL-10 and TNF-alpha in rats with cerebral infarction after transplantation with mesenchymal stem cells. Cell Mol Immunol 2009;6(3):207-13.
28. Johnston IN, Milligan ED, Wieseler-Frank J, Frank MG, Zapata V, Campisi J, et al. A role for proinflammatory cytokines and fractalkine in analgesia, tolerance, and subsequent pain facilitation induced by chronic intrathecal morphine. J Neurosci 2004;24(33):7353-65.
29. Ueland T, Yndestad A, Oie E, Florholmen G, Halvorsen B, Froland SS, et al. Dysregulated osteoprotegerin/RANK ligand/RANK axis in clinical and experimental heart failure. Circulation 2005;111(19):2461-8.
30. Kenedi R. A Textbook of Biomedical Engineering. Glasgow: Blakie & Son; 1980.
31. Schoenau E, Neu CM, Rauch F, Manz F. The development of bone strength at the proximal radius during childhood and adolescence. The Journal of clinical endocrinology and metabolism 2001;86(2):613-8.
32. Liang Y, Seymour RE, Sundberg JP. Inhibition of NF-kappaB signaling retards eosinophilic dermatitis in SHARPIN-deficient mice. J Invest Dermatol 2011; 131(1):141-9.
33. Seymour RE, Hasham MG, Cox GA, Shultz LD, Hogenesch H, Roopenian DC, et al. Spontaneous mutations in the mouse Sharpin gene result in multiorgan inflammation, immune system dysregulation and dermatitis. Genes Immun 2007;8(5):416-21.
34. Schett G. Effects of inflammatory and anti-inflammatory cytokines on the bone. European journal of clinical investigation 2011;41(12):1361-6.
35. Zhang YH, Heulsmann A, Tondravi MM, Mukherjee A, Abu-Amer Y. Tumor necrosis factor-alpha (TNF) stimulates RANKL-induced osteoclastogenesis via coupling of TNF type 1 receptor and RANK signaling pathways. J Biol Chem 2001;276(1):563-8.
36. Novack DV, Faccio R. Osteoclast motility: putting the brakes on bone resorption. Ageing Res Rev 10(1):54-61.
37. Asagiri M, Takayanagi H. The molecular understanding of osteoclast differentiation. Bone 2007;40(2):251-64.
38. Chang J, Wang Z, Tang E, Fan Z, McCauley L, Franceschi R, et al. Inhibition of osteoblastic bone formation by nuclear factor-kappaB. Nat Med 2009; 15(6):682-9.
39. Boyce BF, Yao Z, Xing L. Functions of nuclear factor kappaB in bone. Annals of the New York Academy of Sciences 2010;1192:367-75.
40. Gilbert L, He X, Farmer P, Boden S, Kozlowski M, Rubin J, et al. Inhibition of osteoblast differentiation by tumor necrosis factor-alpha. Endocrinology 2000;141(11):3956-64.
41. Lomaga MA, Yeh WC, Sarosi I, Duncan GS, Furlonger C, Ho A, et al. TRAF6 deficiency results in osteopetrosis and defective interleukin-1, CD40, and LPS signaling. Genes & development 1999;13(8):1015-24.
42. Li J, Sarosi I, Cattley RC, Pretorius J, Asuncion F, Grisanti M, et al. Dkk1-mediated inhibition of Wnt signaling in bone results in osteopenia. Bone 2006; 39(4):754-66.
43. Augat P, Schorlemmer S. The role of cortical bone and its microstructure in bone strength. Age and Ageing 2006; 35(suppl 2):ii27-ii31.
44. Turner CH. Biomechanics of bone: determinants of skeletal fragility and bone quality. Osteoporosis international : a journal established as result of cooperation between the European Foundation for Osteoporosis and the National Osteoporosis Foundation of the USA 2002; 13(2):97-104.
45. Roylance D. Mechanics of Materials. New York: John Wiley & Sons; 1996.